Matemática Contemporânea, Vol. 8, 203–224
http://doi.org/10.21711/231766361995/rmc810

SOME EFFECTS OF VISCOUS TERMS ON RIEMANN PROBLEM SOLUTIONS

Jane M. Hurley **Bradley J. Plohr***

Abstract

This paper concerns 2×2 systems of conservation laws with quadratic fluxes corresponding to Case II in the classification of such problems. Aided by a computer program, we have constructed the solution that satisfies the viscous profile criterion for shock admissibility with respect to a particular choice of viscosity term. Our solution differs from that obtained using the Lax admissibility criterion, even though solutions exist and are unique for both criteria. With the viscous profile criterion, some nonlocal Lax shock waves are inadmissible; in their place, transitional waves appear in the wave patterns.

1. Introduction

In this paper, we present the solutions of Riemann problems for a certain nonlinear 2×2 system of conservation laws:

$$U_t + F(U)_x = 0, \qquad U = \begin{pmatrix} u \\ v \end{pmatrix} \tag{1.1}$$

with initial data

$$U(x,0) = U_0(x) = \begin{cases} U_L & \text{if} \quad x < 0, \\ U_R & \text{if} \quad x > 0. \end{cases} \tag{1.2}$$

*This work was supported in part by: the U. S. Army Research Office under Grant DAAL03-92-G-0185; the U. S. Army Research Office under Grant DAAL03-91-C-0027 to the Mathematical Sciences Institute of Cornell University, through subcontract to Stony Brook; the National Science Foundation under Grant DMS-9201581; the National Science Foundation under Grant INT-9216357; and the Applied Mathematics Subprogram of the U. S. Department of Energy under Grant DE-FG02-90ER25084.

1991 *Mathematics Subject Classification.* 35L65, 35L67

Key words and phrases. Nonlinear non-strictly-hyperbolic conservation laws, Riemann problems, viscous profiles.

We assume that the flux function F is a homogeneous quadratic function in U, and that there is an isolated umbilic point at the origin, where the Jacobian is a multiple of the identity matrix. Away from the origin, the system is strictly hyperbolic, *i.e.*, $F'(U)$ has distinct real eigenvalues $\lambda_1(U) < \lambda_2(U)$. This family of problems has been classified by Schaeffer and Shearer [8] by reducing Eq, (1.1) to the normal form (written in components)

$$\begin{cases} u_t + \frac{1}{2}(au^2 + 2buv + v^2)_x &= 0, \\ v_t + \frac{1}{2}(bu^2 + 2uv)_x &= 0. \end{cases} \tag{1.3}$$

In this paper, we focus on nonsymmetric ($b \neq 0$) models falling into Case II, in which the parameters a and b satisfy the inequality

$$\frac{3}{4}b^2 < a < 1 + b^2. \tag{1.4}$$

For the solutions diagrammed below, $a = 0.5$ and $b = 0.2$. We expect that the solutions obtained using these parameter values are representative of the solutions for any a and b satisfying the inequality (1.4).

Schaeffer and Shearer [9] have solved the Riemann problems (1.1)-(1.2) under the requirement that all shock waves that appear in the solutions satisfy the Lax admissibility criterion. (See also Ref. [6] for the symmetric case, $b = 0$.) These authors find that a unique solution exists for each U_L and U_R. In the present work, we solve the Riemann problems using shock waves that admit viscous profiles with respect to a particular choice of viscosity term. We also obtain existence and uniqueness of solutions, although some of our solutions differ from those for the Lax criterion.

It is well-known that the Lax and viscous profile admissibility criteria lead to different solutions of Riemann problems. For example, for a scalar conservation law with a flux function that is a double well, there are Lax shock waves that do not satisfy the Oleĭnik admissibility condition, which is equivalent to the viscous profile criterion. Similarly, the Lax criterion differs from Liu's criterion [7], which extends Oleĭnik's criterion to systems of conservation laws. In these cases, a saddle-node bifurcation is responsible for breaking a connecting orbit. In the present work, however, a different bifurcation phenomenon is the underlying

mechanism: the occurrence of double separatrix connections, *i.e.*, transitional shock waves.

2. Admissibility Criteria

A (centered) shock wave solution is a discontinuity that propagates at speed s and separates two constant states U_- and U_+. The quantities s, U_-, and U_+ are related by the Rankine-Hugoniot condition

$$-s[U_+ - U_-] + F(U_+) - F(U_-) = 0. \tag{2.1}$$

As is well known, not all shock waves represent physically admissible solutions. In this work, we consider two different admissibility criteria.

2.1. Lax Criterion. For a 2×2 system of conservation laws, the Lax admissibility criterion requires that, of the four characteristics on the two sides of a shock wave, precisely three impinge on the wave. This means that one of the following sets of inequalities is satisfied:

$$s < \lambda_1(U_L), \qquad \lambda_1(U_R) < s < \lambda_2(U_R), \tag{2.2}$$

or

$$\lambda_1(U_L) < s < \lambda_2(U_L), \qquad \lambda_2(U_R) < s, \tag{2.3}$$

where s is the speed of the shock wave. A shock wave satisfying inequalities (2.2) (resp., (2.3)) is called a Lax 1-shock wave (resp., Lax 2-shock wave).

2.2. Viscous Profile Criterion. The viscous profile criterion requires that a shock wave arise as the limit, as $\epsilon \to 0$, of a traveling wave solution to a parabolic equation associated with Eq. (1.1),

$$U_t + F(U)_x = \epsilon[D(U)U_x]_x, \tag{2.4}$$

where $D(U)$ is called the viscosity matrix. Such a traveling wave solution is of the form

$$U(x,t) = \hat{U}\left(\frac{x - st}{\epsilon}\right), \tag{2.5}$$

where $\hat{U}(\xi) \to U_\pm$ as $\xi \to \pm\infty$. To be a solution of Eq. (2.4), $\hat{U}$ must satisfy the ordinary differential equation

$$-s[\hat{U}(\xi) - U_-] + F(\hat{U}(\xi)) - F(U_-) = D(\hat{U}(\xi))\hat{U}'(\xi). \tag{2.6}$$

According to the Rankine-Hugoniot condition (2.1), U_- and U_+ are critical points of the dynamical system (2.6). A shock wave is said to have a viscous profile if there exists an orbit that connects U_- to U_+, and shock waves with viscous profiles are said to be admissible. For 2×2 systems, the question of shock wave admissibility reduces to studying planar dynamical systems and their critical points.

The admissibility of a shock wave depends, in general, on the viscosity matrix $D(U)$. In this work, we make the simplest choice, $D = I$. This choice is not necessarily the best for physical modeling, but it leads to certain mathematical simplifications. For instance, the Lax inequalities determine the types of the critical points U_- and U_+ of the dynamical system (2.6). Furthermore, because $F'(U)$ has real eigenvalues, a generic critical point has one of three types: a repelling node, an attracting node, or a saddle point.

Although the chosen viscosity matrix is very special, and some features of the solution are not generic, we expect that the solution for a more general choice of $D(U)$ has many of the same features as appear in the solution for $D = I$. The solution for a broader class of viscosity matrices is the subject of current research.

3. Construction of the Wave Curves

The solutions presented in this paper are the product of both analytical and numerical work. The numerical work was done using a computer program written by E. Isaacson, D. Marchesin, and B. Plohr.

3.1. Rarefaction Curves. A rarefaction wave is a piecewise smooth, scale-invariant solution $U(x,t) = \tilde{U}(x/t)$ of Eq. (1.1). After substituting $\tilde{U}(x/t)$ into Eq. (1.1), one finds that the construction of an i-rarefaction curve entails

solving for integral curves of the differential equation $\tilde{U}' = r_i(\tilde{U})$, where $r_i(U)$ is a right eigenvector of $F'(U)$. An i-rarefaction wave through U_L is that portion of the i-th integral curve through U_L along which the characteristic speed $\lambda_i(U)$ is increasing. The shape of the integral curves (and hence the rarefaction curves) for our model can be determined analytically (see Ref. [9]).

3.2. Shock Curves. The Hugoniot locus for a fixed state U_L is given by the set of all points U_R that satisfy Eq. (2.1) for some speed s. The Rankine-Hugoniot condition, however, says nothing about the physical relevance of the shock waves that satisfy it. (See Ref.[4] for a listing of shock wave types that can occur for a 2×2 system.) The 1-shock curves (resp., 2-shock curves) are those portions of the Hugoniot loci that satisfy the Lax inequalities (2.2) (resp., (2.3)).

By converting to a polar coordinate system (R, φ) centered at U_L, the Hugoniot locus can be parameterized by the angle φ. The computer program mentioned above uses this parameterization to numerically generate the Hugoniot locus for any point U_L.

3.3. Composite Curves. In Ref. [9], Schaeffer and Shearer prove that the only composite waves that can occur for homogeneous quadratic models are 1-RS-composite and 2-SR-composite waves. A 1-RS-composite wave occurs when a 1-rarefaction curve intersects the inflection locus, *i.e.*, reaches a point where the characteristic speed $\lambda_1(U)$ is no longer increasing. To extend the 1-wave curve past this inflection point, a 1-shock wave that is characteristic on its left side (*i.e.*, $\lambda_1(U_-) = s$) is adjoined to the rarefaction wave, resulting in a composite wave. A 2-SR-composite wave occurs when a 2-shock curve ends at a point U^* because the shock speed coincides with the characteristic speed $\lambda_2(U^*)$. To extend the 2-wave curve past the point U^*, a 2-rarefaction wave is adjoined to the right side of the shock wave, resulting in a composite wave. The computer program uses Newton's method to construct composite waves.

4. Transitional and Overcompressive Waves

Certain shock waves that are admissible under the Lax criterion are also admissible under the viscous profile criterion. For the case $D = I$, Lax 1-shock waves with viscous profiles correspond to connections from repelling nodes to saddle points, and Lax 2-shock waves with viscous profiles correspond to connections from saddle points to attracting nodes. However, not all Lax shock waves possess viscous profiles. Moreover, there are shock waves that do not satisfy the Lax criterion and yet have viscous profiles. In the solutions that follow, such non-Lax shock waves play an important role.

4.1. Transitional Waves. Transitional waves are not associated with a particular characteristic family, but instead occur in a wave pattern lying between a 1-wave group and a 2-wave group. Thus certain Riemann solutions consist of three or more distinct waves. In a Riemann solution for a quadratic model, there is at most one transitional wave group, which is either a transitional rarefaction wave or a transitional shock wave. (See Ref.[3] for greater detail regarding transitional waves.)

Schaeffer and Shearer [9] use transitional rarefaction waves in their solutions for U_L in certain regions (regions $C1$, $C2$, and $C'2$ described below). Transitional rarefaction waves occur when a 2-rarefaction wave is adjoined on its right side by a 1-rarefaction wave. Since the wave speed is given by the eigenvalues $\lambda_i(U)$ of $F'(U)$, such transitional waves can occur only when there are states at which the eigenvalues coincide. In our problem, this occurs only at the umbilic point, $U = 0$. In a region where a transitional rarefaction wave occurs, the solution is as follows. A 1-wave connects U_L to a point U_{M_1} such that the 2-rarefaction wave curve drawn through U_{M_1} intersects the umbilic point. Passing through the umbilic point, the 2-rarefaction curve becomes a 1-rarefaction curve, which is traversed to a second intermediate point U_{M_2}. A 2-wave curve is then taken to a right state U_R.

Transitional shock waves are non-Lax shock waves that nevertheless do pos-

sess viscous profiles. The viscous profile of such a shock wave connects two saddle points. Reference [3] describes the wedge-shaped regions in state space within which such shock waves can occur. (For the transitional shock waves described in this reference, the connecting orbits lie along a straight lines. In the case of homogeneous quadratic models (1.3) with $D = I$, all saddle-saddle connections are of this kind [1], [3] .) When $D = I$, the wedge-shaped transitional regions degenerate and transitional shock waves occur only between a left state U_L on a secondary bifurcation locus and an open interval of right states U_R on the same bifurcation line. Therefore, in a region where a transitional shock wave is required, the solution consists of a 1-wave to a point on the secondary bifurcation line U_{M_1}, followed by a transitional shock wave from U_{M_1} to a point U_{M_2} lying in the transitional interval, and finally a 2-wave from U_{M_2} to U_R. The transitional shock wave, like a 2-shock wave, must have a wave speed greater than that of the wave preceding it.

4.2. Overcompressive Shock Waves. In contrast with Lax shock waves, overcompressive shock waves have all characteristics impinging on the shock, *i.e.*, $\lambda_2(U_R) < s < \lambda_1(U_L)$. For the case $D = I$, an overcompressive shock wave connects a repelling node to an attracting node. Such shock waves form boundaries of U_R regions. For a Riemann solution containing a 1-shock wave followed by a 2-shock wave, it is possible that as U_R is varied along the 2-shock curve, the speed of the second wave becomes coincident with that of the first, at which point the solution consists of a single overcompressive shock wave.

5. Characteristics of the Solution to the Riemann Problem

In general, solutions to Riemann problems consist of a series of waves — rarefaction waves, shock waves, and composite waves — with increasing wave speed, joining a left state U_L to a right state U_R. For a 2×2 system, the result, for a fixed left state U_L, is a diagram representing the various wave combinations required to get from U_L to different right states U_R in state space. As we vary

U_L, the solution diagram also changes; however, for small variations in U_L, the solution is qualitatively the same, *i.e.,* the number and relative positions of each U_R region remains the same. Using the Lax criterion, Schaeffer and Shearer [9] found the regions within which variations in U_L have no qualitative effect on the solution. Because of the homogeneity of the flux function in our problem, these regions are sectors bounded by certain U_L boundary lines. For a general theory of U_L boundaries, we refer to Refs. [9], [5], and [2].

5.1. U_L **Boundaries.** The U_L boundaries for the model of this paper are shown in Figure 5.1 (for the Lax criterion) and Figure 5.2 (for the viscous profile criterion). For clarity, these figures correspond to $a = 0.9$ and $b = 0.8$; this choice enhances the distinction between the lines B and H_2 while keeping the same relative positions of the boundary lines as for $a = 0.5$ and $b = 0.2$, which are the values used in the U_R diagrams below.

The lines marked B consist of points U_L such that the Hugoniot locus of U_L contains a secondary bifurcation point. The lines marked I_k, $k = 1$ or 2, comprise the inflection loci — points where genuine nonlinearity of the system fails, *i.e.,* $\lambda_k'(U)r_k(U) = 0$. The lines marked D_1 represent the 1-family/2-family double sonic locus — points U_L in the plane for which there exists a shock wave to a state U_R with speed s such that $\lambda_1(U_L) = s = \lambda_2(U_R)$. Finally, H_2 marks the 2-family hysteresis locus — points U_L in the plane for which there exists a shock wave to a state U_R with speed s such that $s = \lambda_2(U_R)$ and $U_R \in I_2$. The labeling of the regions A, B, and C is the same as in Ref. [9]. All of these bifurcation loci were generated from analytic formulae by the computer program mentioned above; these formulae are described in the Appendix.

Figure 5.1 illustrates the division of the U_L plane presented by Schaeffer and Shearer [9] using the Lax criterion; it is to be contrasted with the division for the viscous profile criterion, shown in Fig. 5.2. In Ref. [9], the boundary I_1 is omitted; however, in this paper, we consider I_1 to be a U_L boundary. Also, using the viscous profile criterion, the double sonic loci no longer form boundaries, for the following reason. In the context of the Lax criterion, the double

sonic locus is a U_L boundary because moving U_L across it opens a segment of Lax shock waves on the Hugoniot locus. However, these shock waves do not possess viscous profiles. Consequently, there is no qualitative difference in the viscous profile solutions between regions $A2$ and $A3$, nor between regions $A'2$ and $A'3$.

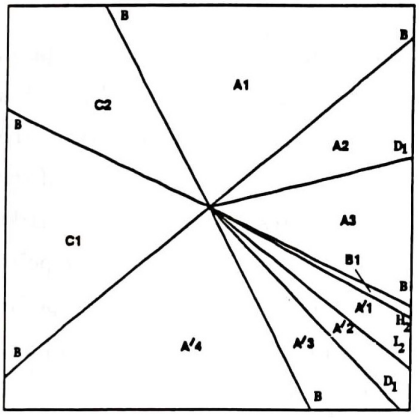

FIGURE 5.1. U_L boundaries using the Lax criterion.

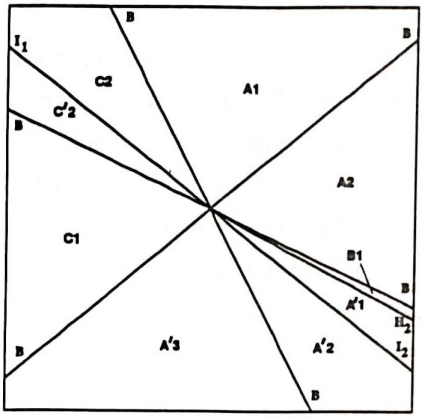

FIGURE 5.2. U_L boundaries using the viscous profile criterion.

Therefore the number of sectors we must consider with the viscous profile criterion is nine. Please note that we have renumbered some of the regions in the viscous profile case. In particular, region $A'3$ in the viscous profile solution corresponds to region $A'4$ in the Lax solution.

5.2. Diagram Legend. In the solution diagrams that follow, we have used

the following notation:

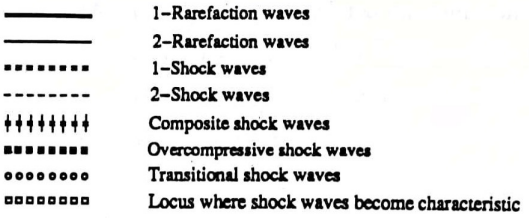

The arrows on the curves indicate the direction of increasing wave speed. A point called B marks the intersection of the Hugoniot curve of U_L with a secondary bifurcation line, and the corresponding point B^* marks where the Hugoniot curve of B bifurcates. A point called C marks the intersection of the 1-rarefaction curve through U_L with D_1, and the corresponding point C^* marks the point reached with a 1-shock wave with characteristic speed from the point C. A point called X marks the point where the nonlocal 1-shock or 1-composite branch is no longer admissible according to the viscous profile criterion. A point called T_R represents the point along the 1-rarefaction branch of U_L from which a transitional rarefaction wave originates.

The point O_{U_L} marks the end of a branch of 2-shock waves from U_L; this shock wave is overcompressive. The point O_B marks where the 2-shock branch from B^* (*i.e.*, one of the branches of the bifurcated Hugoniot locus of B) becomes overcompressive.

The solution diagrams below illustrate the various wave patterns that occur for a fixed left state U_L and an arbitrary right state U_R. The labeling by the letters R, S, and T indicate the series of waves that occur in the Riemann solution when U_R is in that region. For example, RTS denotes a 1-rarefaction wave followed by a transitional shock wave and then a 2-shock wave. The notation (RS) (resp., (SR)) denotes a shock wave that is characteristic on its left (resp., right) side.

6. Solution of the Riemann Problem

6.1. Comparison of Lax and Viscous Profile Solutions. Figures 5.3 and 5.4 show the solutions for a fixed left state U_L in the region $A2$ using the Lax criterion and the viscous profile criterion, respectively. For right states U_R sufficiently close to U_L, the solutions are identical since weak Lax shock waves (*i.e.*, shock waves where $|U_L - U_R|$ is sufficiently small) possess viscous profiles. Strong Lax shock waves, however, do not necessarily have viscous profiles. Part of the Lax solution is constructed using such shock waves with no profiles, *viz.*, certain shock waves that lie on the detached branch of the Hugoniot locus.

First we consider the solution based on the Lax criterion (see Figure 5.3). On the detached branch of the Hugoniot locus, there is a region of 1-shock waves. Extending beyond the 1-shock waves is a segment of composite waves consisting of shock waves that are characteristic on the left. Such waves are constructed by taking a 1-rarefaction wave from the point U_L to a point U_M lying between U_L and C on the 1-wave curve, and following it with a 1-shock wave from U_M to a point in the composite segment, the shock wave having speed $\lambda_1(U_M)$. The entire Lax solution is then constructed by drawing the 2-wave curves that originate from intermediate states on the local branch of the 1-wave curve, the detached branch of the 1-wave curve, and the segment of composite waves. The two small regions near the point C^* labeled SS and $S(SR)$ are distinguished from the larger regions above them with the same labels only because nonlocal Lax 2-shock waves drawn from points on the local 1-wave curve are used in these regions.

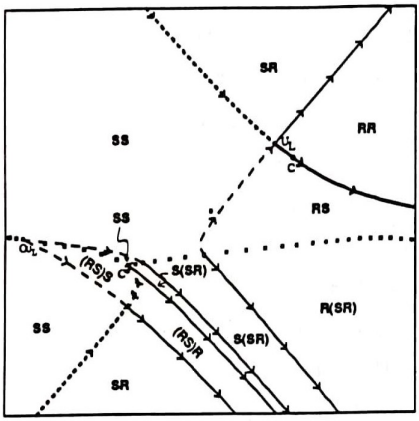

FIGURE 5.3. Lax solution: U_L in region $A2$.

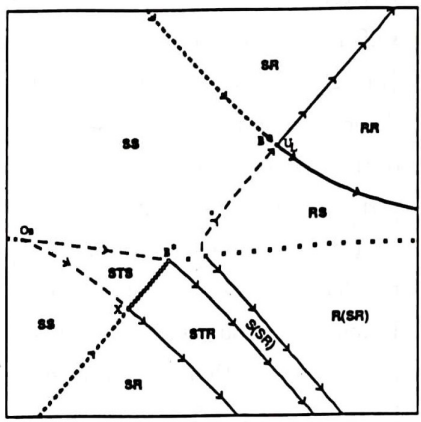

FIGURE 5.4. Viscous profile solution: U_L in region $A2$.

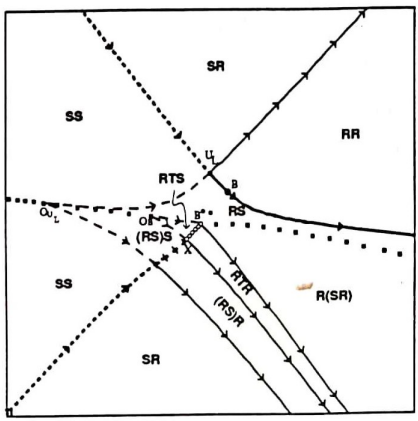

FIGURE 5.5. Viscous profile solution: U_L in region $A1$.

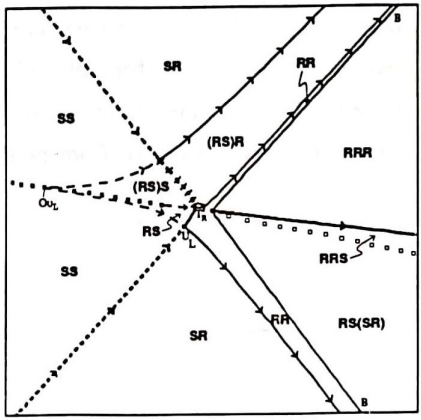

FIGURE 5.6. Viscous profile solution: U_L in region $C1$.

The entire nonlocal 1-shock curve and 1-composite curve is admissible with the Lax criterion, but only a portion of it is admissible with the viscous profile criterion. This nonlocal 1-shock curve intersects a secondary bifurcation line at the point X. For any right state U_R lying on the 1-shock or 1-composite curve extending beyond X, there is no connection from U_L to U_R, hence no viscous profile. Also, of the nonlocal 2-shock waves used to construct the Lax solution, none possess viscous profiles. This occurs because the left state U_L and the segment in question are situated on opposite sides of a secondary bifurcation line. For a right state U_R in a region reached using such a shock wave, both U_L and U_R are critical points of Eq. (2.6); however, there are two other critical points of the system that lie on the secondary bifurcation line separating U_L and U_R. These other critical points are saddle points and there is a connecting orbit between the two. This connection interferes with the one from U_L to U_R. The result is seen in Figure 5.4, where the inadmissible segment is replaced with an interval of transitional shock waves. The entire viscous profile solution is then constructed by drawing the 2-wave curves that originate from intermediate states on the local branch of the 1-wave curve, the admissible portion of the nonlocal 1-wave curve, and the transitional interval. Note that the point C plays no role in the viscous profile solution, since the bifurcation locus D_1 is not a boundary.

The precise structure of the solutions that involve transitional waves depends, in an essential way, on the chosen viscosity matrix $D = I$. (In particular, it is not generic that a single left state B has an interval B^*X of right states that give transitional shock waves.) The result of changing D is the subject of ongoing research.

6.2. Viscous Profile Solution in Remaining Regions. The diagrams for all of the other regions are affected in much the same way, so we describe them only briefly.

As U_L moves across the secondary bifurcation line B into region $A1$, the detached 1-shock branch also crosses B. In contrast with the solution described

above for region $A2$, the entire detached 1-shock curve lies on the same side of B as U_L, so it remains admissible by the viscous profile criterion. Also, a segment of 1-composite waves extends beyond the detached 1-shock curve. Not all of these 1-composite waves are admissible, however. This is because the 1-shock waves with characteristic speeds that originate from intermediate states on the 1-rarefaction branch beyond the point B do not possess viscous profiles; this causes the composite segment to end at the point X. Transitional shock waves are needed to complete the solution, as indicated.

When U_L moves from the A regions to the C regions, there is a fundamental change in the solution. In regions $C1$, $C2$, and $C'2$, a transitional rarefaction wave is necessary to obtain a complete solution (see Figures 5.6, 6.1 and 6.2). For U_R in a region where such a wave is used, the solution is constructed in the following way. First, a 1-wave (rarefaction in $C1$, composite in $C2$, and shock in $C'2$) connects U_L to a point T_R on the transitional rarefaction curve. (This curve coincides with a secondary bifurcation line.) From T_R, the 2-rarefaction curve is traversed up to the umbilic point, where it changes into a 1-rarefaction curve. This 1-rarefaction wave is then traversed to an intermediate state U_M, and a 2-wave curve joins U_M to the right state U_R. In the figures, the lines marked B are secondary bifurcation lines; these lines form the boundary between 2-wave curves originating on the 1-wave curve from U_L and 2-wave curves originating on the transitional rarefaction wave.

The solutions for U_L located in regions A' all share a common feature — the 1-wave curve from U_L intersects the 2-inflection locus at a point I^* (see Figures 6.3, 6.4 and 6.5). The 2-wave curve through I^* creates a U_R boundary, since the orientation of the 2-wave curves is reversed as the intermediate state on the 1-wave curve crosses I_2. In other words, for an intermediate state U_M on one side of this boundary curve, the 2-wave curve through U_M consists of a shock wave in one direction and a rarefaction wave in the other, and these directions are reversed as U_M moves across the boundary curve. The remainder of the solutions in these regions is similar to the solutions in the regions A.

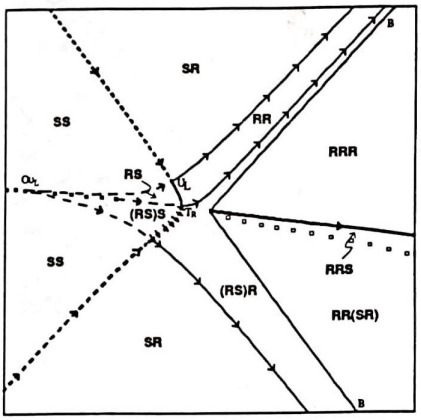

FIGURE 6.1. Viscous profile solution: U_L in region $C2$.

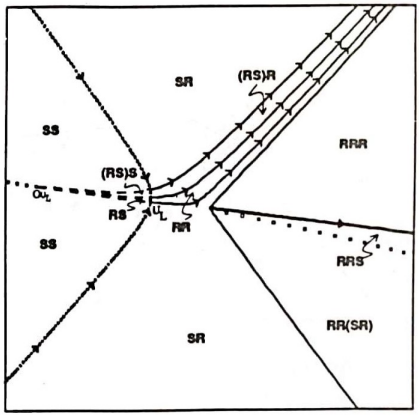

FIGURE 6.2. Viscous profile solution: U_L in region $C'2$.

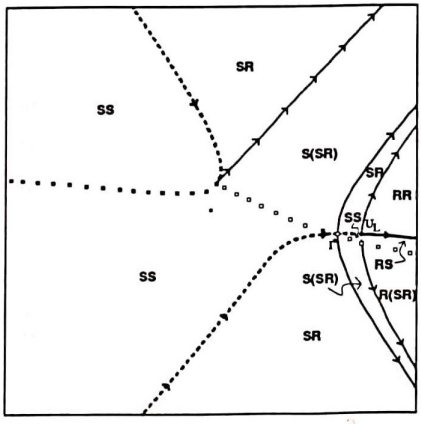

FIGURE 6.3. Viscous profile solution: U_L in region $A'1$.

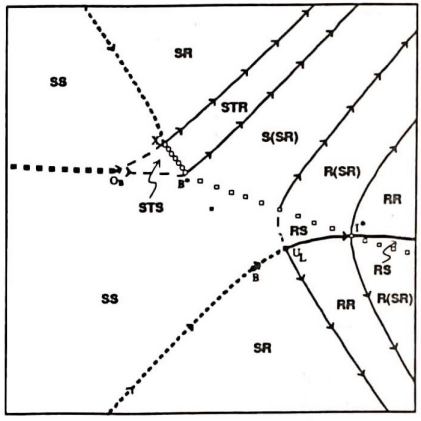

FIGURE 6.4. Viscous profile solution: U_L in region $A'2$.

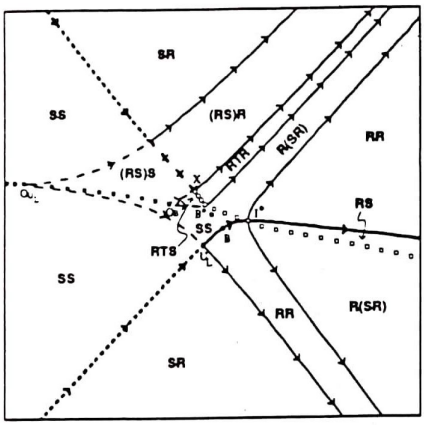

FIGURE 6.5. Viscous profile solution: U_L in region $A'3$.

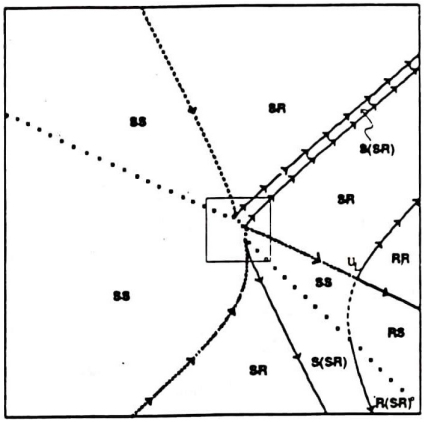

FIGURE 6.6. Viscous profile solution: U_L in region $B1$.

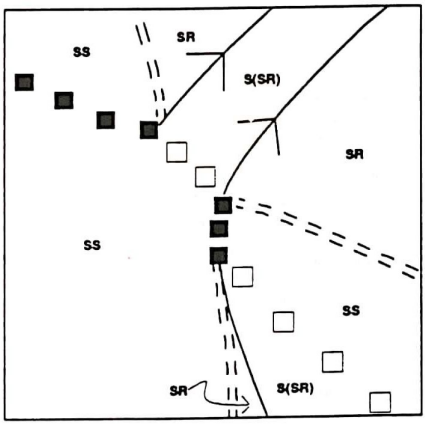

FIGURE 6.7. Viscous profile solution: Blowup of Figure 6.6.

As U_L moves into region $B1$, the local branch of the Hugoniot locus of U_L experiences a secondary bifurcation and a segment of overcompressive shock waves opens up along this branch (Figure 6.6). Away from this overcompressive segment, the solution in region $B1$ is the same as that in region $A'1$. As U_L moves closer to the boundary H_2, the endpoints of this overcompressive segment approach each other and finally coincide when U_L lies on H_2. The box in Figure 6.6 indicates the area that is blown up in Figure 6.7.

7. Conclusion

It is clear that the admissibility criterion plays an important role in the solutions of Riemann problems. Using the viscous profile criterion, we obtain solutions that differ substantially from the Lax solutions. Except for U_L in the C regions, the Lax solution consists solely of combinations of two waves. In the viscous profile solution, however, we must use transitional shock waves to obtain existence throughout the plane, and in these areas, the solution consists of three distinct waves. Thus a significant qualitative feature of the solution (the number of wave groups) is sensitive to the admissibility criterion. One must be careful, therefore, in using a system of conservation laws to model a physical phenomenon, to adopt a criterion that accurately reflects the physics.

In this paper, we have only considered the case $D = I$. This simplifying assumption also leads to behavior that is not generic. In particular, the transitional region is degenerate when D is a multiple of the identity I. Further work in this area will entail looking at the solutions for different choices of viscosity matrix.

Appendix. In Ref. [2], formulae are derived for the bifurcation loci of general systems of conservation laws. These formulae are based on the fundamental wave manifold, which is a regularized solution set for the Rankine-Hugoniot condition. When the wave manifold approach is applied to quadratic models,

one obtains convenient explicit expressions for the bifurcation loci. For such models, points in the wave manifold can be parameterized by $(R, \kappa, \varphi) \in \mathbf{R} \times \mathbf{R} \times (-\pi/2, \pi/2]$ in the following way:

$$u_\pm = u_c(\varphi) - \beta(\varphi)\kappa \pm \frac{1}{2} R \cos\varphi, \tag{7.1}$$

$$v_\pm = v_c(\varphi) + \alpha(\varphi)\kappa \pm \frac{1}{2} R \sin\varphi, \tag{7.2}$$

$$s = \lambda_c(\varphi) + \tilde{\mathcal{D}}(\varphi)\kappa, \tag{7.3}$$

where the coefficient functions α, β, $\tilde{\mathcal{D}}$, λ_c, u_c, and v_c are defined below. The various bifurcation loci are curves in (R, κ, φ)-space, which map to state space via Eqs. (7.1) and (7.2). For homogeneous quadratic models, in fact, these curves comprise connected components in which φ is constant while R and κ lie along a line; the values of φ are roots of homogeneous polynomials in $\cos\varphi$ and $\sin\varphi$. In this appendix, we summarize, without proof, the formulae used in the present paper.

Before we present these formulae, we introduce some notation specific to quadratic models. Consider a general (not necessarily homogeneous) quadratic flux function in U,

$$F(U) = \begin{pmatrix} \frac{1}{2}(a_1 u^2 + 2b_1 uv + c_1 v^2) + d_1 u + e_1 v \\ \frac{1}{2}(a_2 u^2 + 2b_2 uv + c_2 v^2) + d_2 u + e_2 v \end{pmatrix}. \tag{7.4}$$

Associated with such a flux are the following functions (see Ref [3]):

$$\alpha(\varphi) := \frac{1}{2}\{(a_2 + b_1)\cos 2\varphi + (b_2 - a_1)\sin 2\varphi + a_2 - b_1\}, \tag{7.5}$$

$$\beta(\varphi) := \frac{1}{2}\{(b_2 + c_1)\cos 2\varphi + (c_2 - b_1)\sin 2\varphi + b_2 - c_1\}, \tag{7.6}$$

$$\gamma(\varphi) := \frac{1}{2}\{(d_2 + e_1)\cos 2\varphi + (e_2 - d_1)\sin 2\varphi + d_2 - e_1\}, \tag{7.7}$$

$$\tilde{\alpha}(\varphi) := \frac{1}{2}\{(a_1 - b_2)\cos 2\varphi + (b_1 + a_2)\sin 2\varphi + a_1 + b_2\}, \tag{7.8}$$

$$\tilde{\beta}(\varphi) := \frac{1}{2}\{(b_1 - c_2)\cos 2\varphi + (c_1 + b_2)\sin 2\varphi + b_1 + c_2\}, \tag{7.9}$$

$$\tilde{\gamma}(\varphi) := \frac{1}{2}\{(d_1 - e_2)\cos 2\varphi + (e_1 + d_2)\sin 2\varphi + d_1 + e_2\}. \tag{7.10}$$

We also introduce the following functions:

$$\mathcal{D}(\varphi) := \alpha(\varphi)\beta'(\varphi) - \beta(\varphi)\alpha'(\varphi), \tag{7.11}$$

$$\tilde{\mathcal{D}}(\varphi) := \alpha(\varphi)\tilde{\beta}(\varphi) - \beta(\varphi)\tilde{\alpha}(\varphi), \tag{7.12}$$

$$\mu(\varphi) := \alpha(\varphi)\cos\varphi + \beta(\varphi)\sin\varphi, \tag{7.13}$$

$$\tilde{\mu}(\varphi) := \tilde{\alpha}(\varphi)\cos\varphi + \tilde{\beta}(\varphi)\sin\varphi, \tag{7.14}$$

$$\nu(\varphi) := -\alpha(\varphi)\sin\varphi + \beta(\varphi)\cos\varphi, \tag{7.15}$$

$$\tilde{\nu}(\varphi) := -\tilde{\alpha}(\varphi)\sin\varphi + \tilde{\beta}(\varphi)\cos\varphi. \tag{7.16}$$

In these terms, define

$$u_c(\varphi) := -[\gamma(\varphi)\beta'(\varphi) - \beta(\varphi)\gamma'(\varphi)]/\mathcal{D}, \tag{7.17}$$

$$v_c(\varphi) := -[\alpha(\varphi)\gamma'(\varphi) - \gamma(\varphi)\alpha'(\varphi)]/\mathcal{D}, \tag{7.18}$$

$$\lambda_c(\varphi) := \tilde{\alpha}(\varphi)u_c(\varphi) + \tilde{\beta}(\varphi)v_c(\varphi) + \tilde{\gamma}(\varphi). \tag{7.19}$$

It can be shown that: $\mathcal{D}$ and $\tilde{\mathcal{D}}$ are homogeneous quadratic functions of $\cos\varphi$ and $\sin\varphi$; μ, $\tilde{\mu}$, ν, and $\tilde{\nu}$ are homogeneous cubic functions of $\cos\varphi$ and $\sin\varphi$; and

$$\eta := -4\mathcal{D}(\varphi)\{\alpha_0 u_c(\varphi) + \beta_0 v_c(\varphi) + \gamma_0\} \tag{7.20}$$

is independent of φ, the coefficients α_0, β_0, and γ_0 being the terms of $\alpha(\varphi)$, $\beta(\varphi)$, and $\gamma(\varphi)$ that are independent of φ.

For the normal form (1.3), we have $a_1 = a$, $b_1 = b$, $c_1 = 1$, $a_2 = b$, $b_2 = 1$, and all other coefficients equal to zero. Therefore the functions (7.5)–(7.10) simplify to become

$$\alpha(\varphi) = b\cos 2\varphi + \frac{1}{2}(1 - a)\sin 2\varphi, \tag{7.21}$$

$$\beta(\varphi) = \cos 2\varphi - \frac{1}{2}b\sin 2\varphi, \tag{7.22}$$

$$\gamma(\varphi) = 0, \tag{7.23}$$

$$\tilde{\alpha}(\varphi) = \frac{1}{2}(a-1)\cos 2\varphi + b\sin 2\varphi + \frac{1}{2}(a+1), \tag{7.24}$$

$$\tilde{\beta}(\varphi) = \frac{1}{2}b\cos 2\varphi + \sin 2\varphi + \frac{1}{2}b, \tag{7.25}$$

$$\tilde{\gamma}(\varphi) = 0. \tag{7.26}$$

Also, $\mathcal{D}(\varphi) \equiv a - b^2 - 1$ is a constant, $(u_c(\varphi), v_c(\varphi)) \equiv (0,0)$, and $\eta = 0$.

The (right-sided) secondary bifurcation locus is obtained as follows. First find the values of φ such that $\mu(\varphi) = 0$; there are up to three roots of this homogeneous cubic function. Then each root corresponds to a branch of the secondary bifurcation locus, namely the line along which R and κ satisfy $\mathcal{D}(\varphi)\kappa + \frac{1}{2}\nu(\varphi)R = 0$. In the case of the normal form, the equation for φ is

$$\sin^3\varphi + 2b\sin^2\varphi\cos\varphi + (a-2)\sin\varphi\cos^2\varphi - b\cos^3\varphi = 0, \tag{7.27}$$

which has three distinct solutions in Case II.

The inflection locus comprises points in the surface $R = 0$ for which κ and φ satisfy

$$[\tilde{\mu}(\varphi)\mathcal{D}(\varphi) + \frac{1}{2}\mu(\varphi)\mathcal{D}'(\varphi)]\kappa - \frac{1}{2}\mu(\varphi)\eta/\mathcal{D}(\varphi) = 0. \tag{7.28}$$

For the normal form, this means that $\tilde{\mu}(\varphi) = 0$ and κ is arbitrary. The requirement on φ reduces to

$$\cos\varphi\left(3\sin^2\varphi + 3b\sin\varphi\cos\varphi + a\cos^2\varphi\right) = 0. \tag{7.29}$$

This equation has only one solution, $\varphi = \pi/2$, in Case II.

For points on the double sonic locus, R is arbitrary, $\tilde{\mathcal{D}}(\varphi) = 0$, and Eq. (7.28) is satisfied. In the case of the normal form, κ must be zero, and the equation $\tilde{\mathcal{D}}(\varphi) = 0$ can be expressed as

$$\sin^2\varphi + b\sin\varphi\cos\varphi + (b^2 - a)\cos^2\varphi = 0. \tag{7.30}$$

There are two distinct solutions φ in Case II.

The (R, κ, φ)-coordinates of points on the (right-sided) hysteresis locus satisfy the system of equations

$$-\frac{1}{2}\tilde{\mathcal{D}}(\varphi)R + [\tilde{\mu}(\varphi)\mathcal{D}(\varphi) + \frac{1}{2}\mu(\varphi)\mathcal{D}'(\varphi)]\kappa - \frac{1}{2}\mu(\varphi)\eta/\mathcal{D}(\varphi) = 0, \tag{7.31}$$

$$-\frac{1}{4}\tilde{\mathcal{D}}'(\varphi)R + [\tilde{\nu}(\varphi)\mathcal{D}(\varphi) + \frac{1}{2}\nu(\varphi)\mathcal{D}'(\varphi)]\kappa - \frac{1}{2}\nu(\varphi)\eta/\mathcal{D}(\varphi) = 0. \tag{7.32}$$

In the case of the normal form, Eqs.(7.31) and (7.32) reduce to

$$-\frac{1}{2}\tilde{\mathcal{D}}(\varphi)R + \tilde{\mu}(\varphi)\mathcal{D}(\varphi)\kappa = 0, \tag{7.33}$$

$$-\frac{1}{4}\tilde{\mathcal{D}}'(\varphi)R + \tilde{\nu}(\varphi)\mathcal{D}(\varphi)\kappa = 0. \tag{7.34}$$

For Eqs. (7.33) and (7.34) to have a nontrivial solution, φ must satisfy

$$\tilde{\mathcal{D}}(\varphi)\tilde{\nu}(\varphi) - \frac{1}{2}\tilde{\mathcal{D}}'(\varphi)\tilde{\mu}(\varphi) = 0; \tag{7.35}$$

this equation can be written

$$2\sin^3\varphi + 3b\sin^2\varphi\cos\varphi + (6a - 3b^2)\sin\varphi\cos^2\varphi + (3ab - 2b^3)\cos^3\varphi = 0. \tag{7.36}$$

There is only one solution φ of this equation in Case II, and for this value for φ, there is a one-dimensional solution set of the linear equations (7.33) and (7.34).

References

[1] C. Chicone, *Quadratic gradients on the plane are generically Morse-Smale*, J. Differential Equations **33** (1979), 159–166.

[2] E. Isaacson, D. Marchesin, C. F. Palmeira, and B. Plohr, *A global formalism for nonlinear waves in conservation laws*, Comm. Math. Phys. **146** (1992), 505–552.

[3] E. Isaacson, D. Marchesin, and B. Plohr, *Transitional waves for conservation laws*, SIAM J. Math. Anal. **21** (1990), 837–866.

[4] E. Isaacson, D. Marchesin, B. Plohr, and J. B. Temple, *The Riemann problem near a hyperbolic singularity: the classification of quadratic Riemann problems I*, SIAM J. Appl. Math. **48** (1988), 1009–1032.

[5] ——, *Multiphase flow models with singular Riemann problems*, Mat. Aplic. Comput. **11** (1992), 147–166.

[6] E. Isaacson and J. B. Temple, *The Riemann problem near a hyperbolic singularity III*, SIAM J. Appl. Math. **48** (1988), 1302–1312.

[7] T.-P. Liu, *The Riemann problem for general* 2×2 *conservation laws*, Trans. Amer. Math. Soc. **199** (1974), 89–112.

[8] D. Schaeffer and M. Shearer, *The classification of* 2×2 *systems of nonstrictly hyperbolic conservation laws, with application to oil recovery*, Comm. Pure Appl. Math. **40** (1987), 141–178.

[9] ——, *Riemann problems for nonstrictly hyperbolic* 2×2 *systems of conservation laws*, Trans. Amer. Math. Soc. **304** (1987), 267–306.

Department of Applied Mathematics
and Statistics
State University of
New York at Stony Brook
Stony Brook, NY 11794-3600
Email: hurley@ams.sunysb.edu

Departments of Mathematics and of
Applied Mathematics and Statistics
State University of
New York at Stony Brook
Stony Brook, NY 11794-3600
Email: plohr@ams.sunysb.edu